

Effect of sulphur on the strengthening of a Zr–Nb alloy

K.I. Chang, S.I. Hong *

Chungnam National University, Department of Metallurgical Engineering, Taedok Science Town, Taejeon 305-764, Republic of Korea

Received 22 November 2006; accepted 21 April 2007

Abstract

The effect of sulphur on the strengthening and the thermally activated deformation of cold-worked Zr–1 Nb alloy was investigated. In the present study, the sulphur strengthening was observed even at room temperature unlike the previous study of Ferrer et al. The flow stress increased by 65 MPa at room temperature with the addition of sulphur as little as 20 ppm. With further increase of sulphur content up to 300 ppm, negligible change of the flow stress was observed. The additive strengthening behavior in which the entire stress–strain curve shift upward by the friction stress due to the addition of sulphur was observed in the Zr–Nb alloy of the present study. The activation volume decreased slightly (from $110b^3$ to $80b^3$) with the addition of 300 ppm sulphur at room temperature. The rate-controlling mechanism of the deformation can best be explained by the dislocation interaction mechanism in which the segregation of alloying elements such as oxygen and sulphur atoms affects the activation length of dislocations.

© 2007 Elsevier B.V. All rights reserved.

1. Introduction

Sulphur and phosphorus have been known to cause the embrittlement in many alloys by reducing the boundary cohesive strength [1–5]. The effect of sulphur and phosphorus have been extensively studied and various models have been proposed to account for the reduction of the cohesive strength [4–8]. A surprising result that the thermal creep resistance can be improved drastically by the addition of sulphur as little as 10 ppm [9] has almost been unnoticed outside the nuclear industry and the nuclear-related academic community. The addition of 25 wt% ppm sulphur is known to be enough to reduce the creep rate of zirconium alloys by a factor of three at 400 °C [9,10]. Charquet [11] also reported that sulphur has an extremely beneficial effect on the steam corrosion resistance in zirconium alloys at 400 °C. Despite the significant beneficial effect of sulphur on the creep resistance of zirconium alloys reported by Charquet et al. [9], not much attention has been paid to the beneficial effects of sulphur in zirconium alloys. Nevertheless, sulphur containing zirconium alloys have been patented [10,12] and commercialized.

Ferrer et al. [10] investigated the effect of sulphur on the plasticity of zirconium alloys. They [10] suggested that the sulphur strengthening effect has similarities to the oxygen strengthening effect in zirconium alloys. However, they concluded that there are also differences between the two elements and the sulphur and oxygen effects are independent from each other [11]. They proposed that the sulphur segregation at dislocation cores can modify the dislocation core, which in turn would affect the mobility of dislocations. However, the modification of the dislocation core over the meaningful length of the dislocation in a Zr–Nb alloy containing sulphur as little as 25 ppm is questionable. The beneficial effects of sulphur in zirconium alloys have been reported only by investigators of a zirconium tube manufacturer that commercialized the sulphur containing zirconium alloy tubes. This study was aimed at not only understanding the strengthening mechanism of sulphur but also confirming the strengthening effect of sulphur.

2. Experimental

A Zr–1 wt% Nb alloy without sulphur addition and Zr–1 wt% Nb with various sulphur contents were cast by vacuum arc melting. The addition of sulphur was made

* Corresponding author.

E-mail address: sihong@cnu.ac.kr (S.I. Hong).

Table 1
Activation volume V^* and the strain rate sensitivity m of Zr–Nb and Zr–Nb–S alloys

	V^*		m	
	Room temperature	300 °C	Room temperature	300 °C
Zr–1.0 wt% Nb	$1.09 \times 10^2 b^3$	$2.68 \times 10^2 b^3$	0.011	0.011
Zr–1.0 wt% Nb–300 ppm S	$7.61 \times 10^1 b^3$	$2.07 \times 10^2 b^3$	0.013	0.014

by adding iron sulfide in the melt. The buttons were annealed (850 °C/1 h), β -quenched, hot-rolled at 580 °C, annealed at 600 °C and cold-rolled into 1 mm thick plates with an intermediate annealing at 600 °C. The reduction of the thickness during cold rolling was 75%. Tensile testing was performed using a united testing machine (SFP 10) equipped with a three-zone furnace at room temperature and at 300 °C.

Strain jump tests were performed at room temperature and 300 °C to obtain the activation volume and the strain rate sensitivity for Zr–1.0Nb and Zr–1.0Nb–300 ppm S and the results are summarized in Table 1. The samples were initially strained at the strain rate of 10^{-4} /s and the strain rate was changed to 10^{-2} /s at the plastic strain of 0.1.

3. Experimental results

Fig. 1(a)–(c) shows the TEM micrographs of Zr–1.0Nb, Zr–1.0Nb–100 ppm S and Zr–1.0Nb–300 ppm S (before tensile testing), respectively. Dislocation tangles and networks introduced during the thermo-mechanical processing are shown. EDS analysis revealed that small round particles in Fig. 1 are Fe containing intermetallics. No appreciable sulphur peaks were observed in the particles as well as in the matrix. X-ray diffraction pattern analysis did not display any peak from sulphur containing compounds such as iron sulfide, zirconium sulfide and niobium sulfide (not shown), which is likely due to the low sulphur content.

The stress–strain responses of Zr–1.0Nb with various sulphur contents at room temperature and 300 °C are shown in Fig. 2(a) and (b), respectively. The flow stress increased by 65 MPa at room temperature with the addition of sulphur as little as 20 ppm. With further increase of sulphur content up to 300 ppm, negligible change of the flow stress was observed. The elongation decreased with the increase of the sulphur content, but the reduction of the ductility with the addition of 20 ppm sulphur is insignificant. At 300 °C, the flow stress also increased by \sim 60 MPa with the addition of 20 ppm sulphur and no appreciable change of the flow stress was observed with further increase of sulphur. At 300 °C, however, the effect of sulphur on the ductility was insignificant.

The strength level of Zr–Nb of the present study is far higher than that of Ferrer et al. [10] because of the different thermo-mechanical processing. The yield stress of Zr–Nb

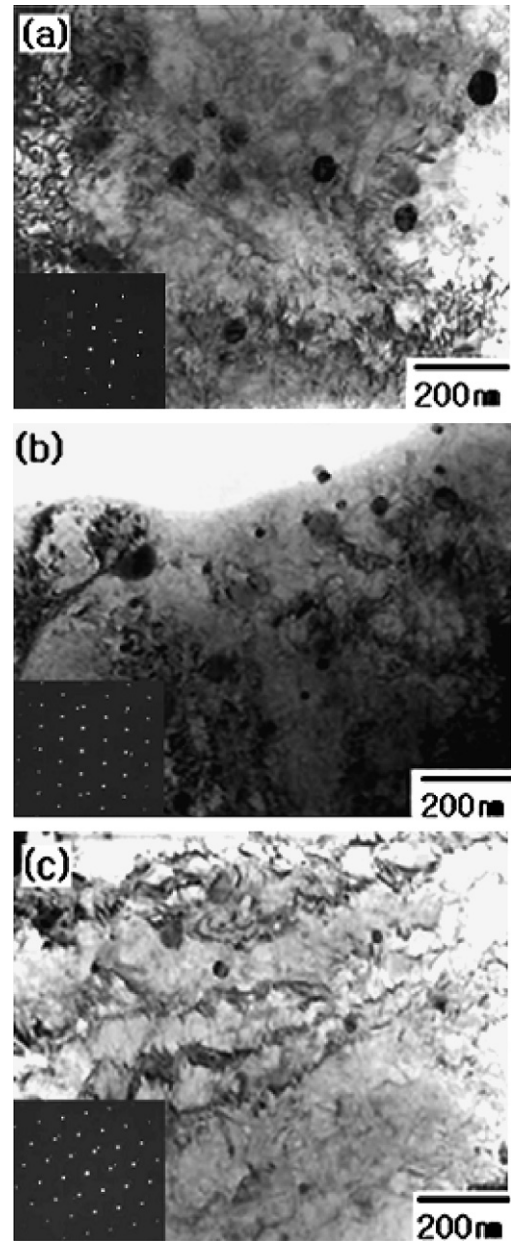


Fig. 1. TEM micrographs of as-cold-rolled Zr–1.0Nb (a), Zr–1.0Nb–100 ppm S (b) and Zr–1.0Nb–300 ppm S (c).

alloy of Ferrer et al. [10] is 50 MPa at 200 °C because it was annealed in the final stage of thermo-mechanical processing whereas that of the present study is 370 MPa at 300 °C. In Zr–Nb alloy of the present study, the flow strengthening after the yielding is far less significant than that of Ferrer et al. [10] and flow softening is dominant after the peak stress. The high strength and the dominant flow softening after initial brief strengthening reflect the higher stored cold work during the thermo-mechanical processing of the present alloy. One interesting observation is that the sulphur strengthening was observed even at room temperature in the present study unlike the observation of Ferrer et al. [10]. They [10] reported that the sulphur strengthening appeared at about 100 °C and was maximal

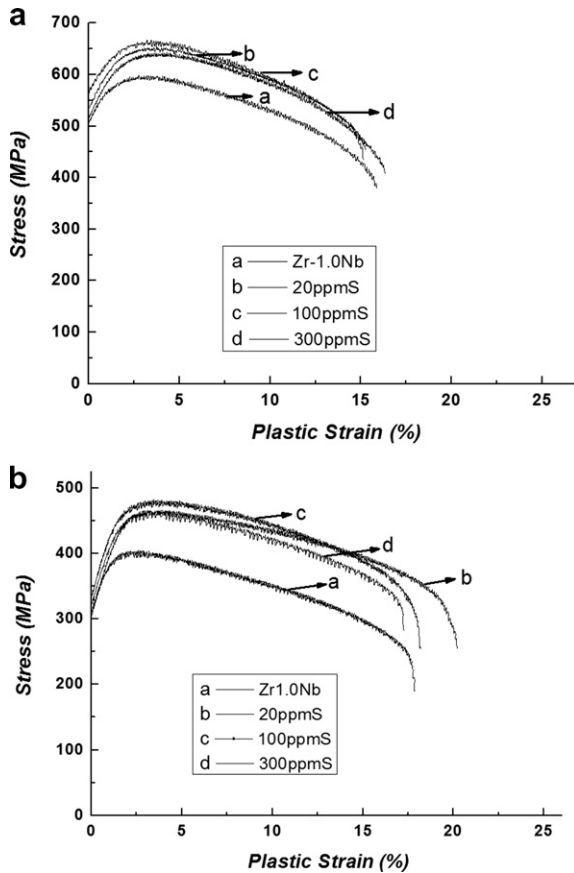


Fig. 2. Stress–strain responses of Zr–1.0Nb with various sulphur contents at room temperature (a) and 300 °C (b).

at around 400 °C with the stress increment of 25 MPa. Another different strengthening behavior in the Zr–Nb alloy of the present study is the additive strengthening in which the entire stress–strain curve shift upward by the friction stress compared to the multiplicative strengthening [13] in which the stress–strain curves diverge with increasing strain in Zr–Nb alloy of Ferrer et al. [10].

Fracture surfaces of Zr–1.0Nb (a), Zr–1.0Nb–100 ppm S (b) and Zr–1.0Nb–300 ppm S (c) after tensile testing at room temperature are displayed in Fig. 3. All alloys exhibited ductile fracture surfaces, supporting beneficial effect of sulphur in zirconium alloys. It is obvious that sulphur does not cause any embrittlement in Zr and Zr base alloys. The similar ductile fracture surfaces were observed at 300 °C for all alloys with sulphur.

In order to investigate the deformation mechanism of Zr–Nb alloys, the activation volume for plastic flow was measured. The activation volume V^* associated with the deformation process has been obtained from the following equation [14,15]:

$$V^* = kT \partial \ln \dot{\gamma} / \partial \tau = nkT \ln(\dot{\epsilon})_1 / (\dot{\epsilon})_2 / (\sigma_1 - \sigma_2),$$

where k is the Boltzmann constant, $\dot{\gamma}$ is the shear strain rate, σ_1 and σ_2 are the applied shear stresses at the normal strain rates $(\dot{\epsilon})_1$ and $(\dot{\epsilon})_2$ and T is the absolute temperature. The shear stress τ was calculated from the normal flow

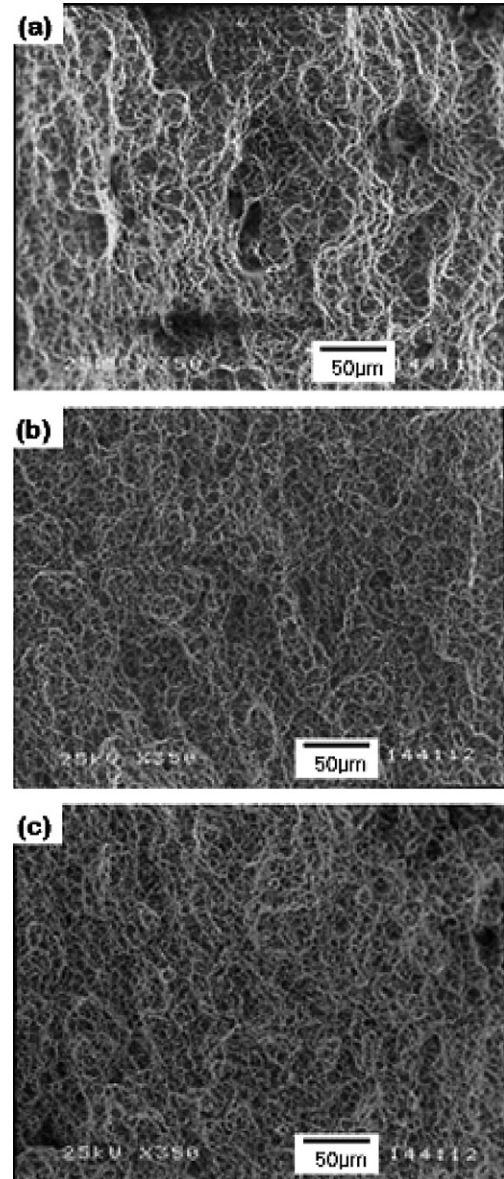


Fig. 3. Fracture surfaces of Zr–1.0Nb (a), Zr–1.0Nb–100 ppm S (b) and Zr–1.0Nb–300 ppm S (c) after tensile testing at room temperature.

stress σ , using the relation $\tau = \sigma/m$, where n is the Taylor factor. According to Luton and Jonas, m is assumed to be equal to 4 [16]. Strain jump tests were performed at room temperature and for Zr–1.0Nb and Zr–1.0Nb–300 ppm S 300 °C to obtain the activation volume and the strain rate sensitivity and the results are summarized in Table 1. The activation volume, V^* , decreased from $110b^3$ to $80b^3$ where b is the Burgers vector and the strain rate sensitivity, m , increased slightly from 0.0111 to 0.0127 with the addition of 300 ppm sulphur at room temperature. At 300 °C, the activation volume decreased slightly from $270b^3$ to $200b^3$ with the addition of 300 ppm sulphur. The activation volume obtained at room temperature in Zr–1.0Nb–300 ppm S of the present study ($80b^3$) is a little larger than that ($40b^3$) observed by Ferrer et al. [10] on α -zirconium containing 25 ppm sulphur.

4. Discussion

The observation that sulphur has the strengthening effect at a lower temperature (room temperature) in the present study than the study (100 °C) of Ferrer et al. [10] can be associated with the difference of the dislocation density. The alloys in the study of Ferrer et al. [10] were fully annealed after thermo-mechanical processing, and the dislocation density is low. The alloys of the present study were cold-rolled with intermediate heat treatments, and the dislocation density was observed to be high as shown (dislocation tangles and networks) in Fig. 1. The diffusivity increases with the increase of dislocation density and the effect of solute atoms could appear at lower temperatures in Zr alloys with higher dislocation density as shown in this study.

The difference of the strain dependence on strengthening (the additive strengthening in the present study and the multiplicative strengthening in Zr–Nb alloy of Ferrer et al. [10]) can also be attributed to the difference of the dislocation density. The multiplicative strengthening in which strain hardening increases more rapidly with the solute content is caused by the interaction between solution hardening and strain hardening [13]. Since strain hardening is mostly associated with the increasing dislocation density with strain, the multiplicative strengthening behavior intensifies in materials with strong strain hardening behavior. In Zr–Nb alloys of the present study, the initial dislocation density is high because of high cold work energy and the equilibrium state can be reached in the early stage of deformation by a balance between strain hardening and dynamic recovery. Therefore, the interaction between solution hardening and strain hardening is minimal and the stress–strain curves differ only by the same frictional stress caused by solute atoms as shown in Fig. 2.

The basic rate-controlling mechanisms that could be operative in Zr–Nb alloys with or without sulphur are (1) intersection of dislocations ($V^* = 10^3\text{--}10^4b^3$ when the dislocation density is lower than 10^9 cm^{-2} , $V^* < 10^2b^3$ when the dislocation density is higher than 10^{11} cm^{-2}), (2) Peierls–Nabarro force ($V^* = 10\text{--}10^2b^3$), (3) non-conservative motion of jogs ($V^* = 10^2\text{--}10^4b^3$), (4) cross-slip ($V^* = 10\text{--}10^2b^3$ depending on stacking fault energy), (5) overcoming of solute atoms by dislocation ($V^* = 1\text{--}10^3b^3$ depending on the concentration of solute atoms).

Hong et al. [15] suggested that the possible rate-controlling mechanism of zirconium alloys should explain the dependence of the activation volume on the microstructural scale dependent on the deformation processing. The activation volume due to non-conservative motion of jogs cannot be lower than 10^2b^3 because the density of jogs reaches the saturation through annihilation of vacancy-producing jogs and interstitial-producing jogs [10,14]. Hong et al. [15] suggested that the most probable rate-controlling mechanism of Zircaloy was the interaction of dislocations and segregated solutes at dislocations. It was suggested by Hong et al. [15] that the Peierls–Nabarro force and cross-slip could not be the rate-controlling

mechanism for deformation of Zr and Zr alloys since the Peierls–Nabarro force and cross-slip are not dependent on the deformation processing history [14,15]. The activation volumes associated with Peierls–Nabarro force and cross-slip is not sensitive to the dislocation density [10,14,15].

Kocks suggested that the activation length (described as ‘bulge length’ in the paper of Kocks [13]) is affected by the segregated alloying elements although the maximum bulge length is limited by the forest spacing. The interaction between strain hardening and solution hardening, including strain aging, all observed in Zr base alloys, can be easily explained by the model of Kocks [13]. It was suggested by Kocks [13] that the segregation of solute atoms at dislocations makes a great contribution to solution strengthening even below the temperature range of dynamic strain aging. Dislocations can collect a significant number of solute atoms from its surroundings after being stopped by forest dislocations [13,17] at low temperatures. Indeed, Hong and Laird [18] and Kocks [13] suggested the similarity between the solution strengthening behavior at low temperatures and the dynamic strain aging behavior at intermediate temperatures. It is well known that the dynamic strain aging at intermediate temperatures in zirconium alloys is caused by the interaction of dislocations and oxygen atoms [19–22]. The element which can be segregated at dislocations and affects the thermal activation process at low temperatures is thought to be oxygen atoms in most Zr alloys. Oxygen atoms can segregate easily at dislocations (even at room temperature) while dislocations wait for thermal activation after being stopped at forest dislocations and can contribute to solution strengthening [13,17].

The segregation of sulphur atoms to dislocations can result in the slight decrease of the activation volume and the increase of the strength. To examine the effect of sulphur on the strength, the effect of sulphur on the thermally activated deformation mechanism should be discussed. Ferrer et al. [10] examined the effect of sulphur on the plastic deformation of Zr–Nb and tried to explain the origin of sulphur effect. They [10] suggested that sulphur interacted with dislocations and the mechanism controlling the deformation kinetics is a dislocation mechanism. They [10] also suggested that sulphur does not act as a fixed obstacle, but as a mobile one, resulting in the appreciable increase of the strength with the minimal addition of sulphur. They [10] concluded that sulphur, although it has similarities to the oxygen hardening effect, strengthen the Zr alloy by the modification of dislocation cores. Ferrer et al. [10] suggested that sulphur segregation at dislocation core could modify the core structure of dislocations, which would affect most of the dislocation properties including Peierls friction, cross-slip, pipe diffusion and interaction with other impurities.

The model of Ferrer et al. [10] on the effect of sulphur strengthening, however, does not appear to have a sound basis. For the modification of dislocation cores by sulphur to be an operative strengthening mechanism, the dislocation cores should be modified over a reasonable length of

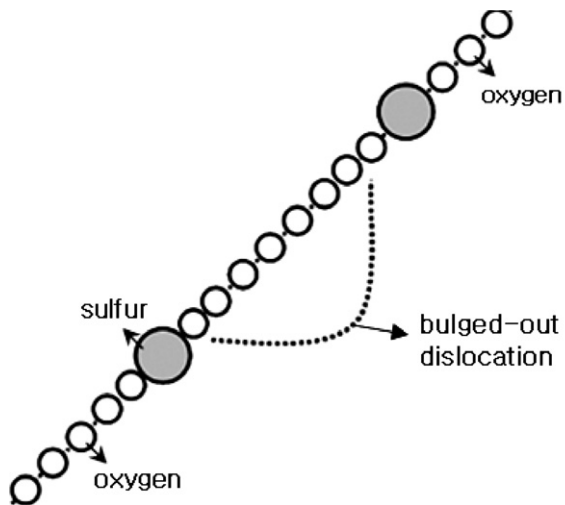


Fig. 4. Thermally activated nucleation of a bulge from a dislocation decorated with solute atoms.

dislocations with the modified core structure maintained while they are in motion during deformation.

The presence of sulphur atoms as little as 20 ppm is not likely to modify the dislocation cores over the reasonable length of dislocations. Furthermore, it is questionable if the mobility of sulphur atoms is high enough to keep up with moving dislocations to maintain the modified dislocation core structure during deformation. In Ferrer's model, if the dislocations are liberated from the segregated sulphur atoms, the modified core structure would return to its original structure and the Peierls friction may not be appreciable. It is more likely that sulphur atoms pin a segment of dislocations by segregating at dislocations or occupying relaxed octahedral sites [19] adjacent to dislocations just like the oxygen atoms [20–23]. In this case, oxygen and sulphur atoms have the additive strengthening effect as supported by the observation of Ferrer et al. [10] that the dynamic strain aging effects such as the athermal plateau, the age hardening peak and low strain sensitivity intensified with the addition of sulphur. Ferrer et al. [10] concluded that the sulphur and oxygen effects are independent and the natures of these two effects are different although they are supplementary to each other.

The interaction of oxygen and sulphur atoms with a dislocation and its effect on activation of bulge can be schematically depicted in Fig. 4. The segregation of sulphur atoms in addition to oxygen atoms could decrease the activation volume by limiting the length of the activated bulge and enhance the strengthening effect. The effect of sulphur atoms, although the concentration is very small, can be appreciable because the size of sulphur atoms is much larger than that of oxygen atoms.

5. Conclusions

On the basis of the investigation of the effect of sulphur on the strengthening and the activation volume, the following conclusions can be drawn:

1. The sulphur strengthening was observed even at room temperature unlike the previous study of Ferrer et al. The flow stress increased by 65 MPa at room temperature with the addition of sulphur as little as 20 ppm. The appearance of the sulphur effect at lower temperature can be attributed to a higher dislocation density in the cold-worked Zr–1 Nb.
2. The additive strengthening behavior in which the entire stress–strain curve shifts upward by the friction stress due to the addition of sulphur was observed in Zr–Nb alloy of the present study. The difference of the strain dependence of the strengthening (the additive strengthening in the present study and the multiplicative strengthening in Zr–Nb alloy of Ferrer et al. [10]) can also be attributed to the difference of the dislocation density.
3. The activation volume decreased from $110b^3$ to $80b^3$ where b is the Burgers vector and the strain rate sensitivity increased slightly from 0.0111 to 0.0127 with the addition of 300 ppm sulphur at room temperature. At 300 °C, the activation volume decreased slightly from $270b^3$ to $200b^3$ with the addition of 300 ppm sulphur.
4. The elongation decreased with the increase of the sulphur content, but the reduction of the ductility with the addition of 20 ppm sulphur is insignificant at room temperature. All alloys containing sulphur up to 300 ppm exhibited ductile fracture surfaces, supporting sulphur does not cause any embrittlement in Zr and Zr base alloys.
5. The rate-controlling mechanism of the deformation can best be explained by the dislocation interaction mechanism in which the segregation of alloying elements such as affects the activation length of dislocations. The segregation of sulphur atoms in addition to oxygen atoms could decrease the activation volume by limiting the length of the activated bulge and enhance the strengthening effect.

Acknowledgement

The authors acknowledge the support from MOCIE (Ministry of Commerce, Industry and Energy), funded through Korea Nuclear Fuel Co. (2006).

References

- [1] P. Rez, J.R. Alvarez, *Acta Mater.* 47 (2006) 4069.
- [2] D. Bika, C.J. McMahon Jr., *Acta Metall. Mater.* 43 (1995) 1909.
- [3] J.K. Heuer, P.R. Okamoto, N.Q. Lam, J.F. Stubbins, *J. Nucl. Mater.* 301 (2002) 129.
- [4] R.D.K. Misra, *Acta Mater.* 44 (1996) 4367.
- [5] Z.F. Hu, Z.G. Yang, *Mater. Sci. Eng. A.* 383 (2004) 224.
- [6] R.P. Messmer, C.L. Briant, *Acta Metall.* 30 (1982) 457.
- [7] R.J. Haydock, *Physica C* 14 (1981) 3807.
- [8] R. Wu, A.J. Freeman, G.B. Olson, *Science* 265 (1994) 376.
- [9] D. Charquet, J. Senevat, J.P. Marcon, *J. Nucl. Mater.* 255 (1998) 78.
- [10] F. Ferrer, A. Barbu, T. Bretheau, J. Crepin, F. Willaime, D. Charquet, in: G.D. Moan, P. Rudling (Eds.), 13th International

- Symposium on Zirconium in the Nuclear Industry, ASTM STP 1423, 2002, p. 863.
- [11] D. Charquet, *J. Nucl. Mater.* 304 (2002) 246.
- [12] D. Charquet, Zirconium-based alloy, manufacturing process, and use in a nuclear reactor, US Patent 5832050, 1998.
- [13] U.F. Kocks, *Metall. Trans.* 16A (1985) 2109.
- [14] H. Conrad, *J. Met.* 16 (1964) 582.
- [15] S.I. Hong, K.W. Lee, K.T. Kim, *J. Nucl. Mater.* 303 (2002) 169.
- [16] M.J. Luton, J.J. Jonas, *Can. Metal. Quart.* 11 (1972) 79.
- [17] Z.S. Basinski, R.A. Foxall, R. Pascual, *Scripta Metall.* 6 (1972) 807.
- [18] S.I. Hong, C. Laird, *Acta Metall. Mater.* 38 (1990) 1581.
- [19] J.L. Snoek, *Physica* 8 (1941) 711.
- [20] S.I. Hong, *Scripta Mater.* 44 (2001) 995.
- [21] S.I. Hong, W.S. Ryu, C.S. Rim, *J. Nucl. Mater.* 120 (1984) 1.
- [22] S.I. Hong, W.S. Ryu, C.S. Rim, *J. Nucl. Mater.* 116 (1983) 314.
- [23] J.L. Derep, S. Ibrahim, R. Rouby, G. Fantozzi, *Acta Metall.* 28 (1980) 607.